

Linear Viscoelasticity of Polyelectrolyte Complex Coacervates

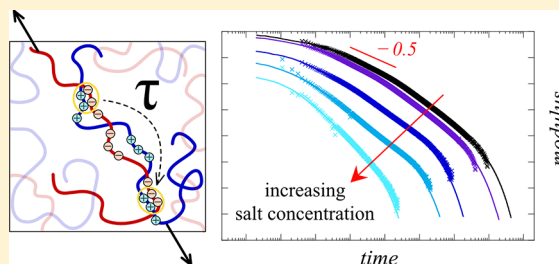
Evan Spruijt, Martien A. Cohen Stuart, and Jasper van der Gucht*

Laboratory of Physical Chemistry and Colloid Science, Wageningen University, Dreijenplein 6, 6703 HB Wageningen, The Netherlands

S Supporting Information

ABSTRACT: Two flexible, oppositely charged polymers can form liquid-like complex coacervate phases with rich but poorly understood viscoelastic properties. They serve as an experimental model system for many biological and man-made materials made from oppositely charged macromolecules. We use rheology to systematically study the viscoelastic properties as a function of salt concentration, chain length, chain length matching, and mixing stoichiometry of model complex coacervates of poly(*N,N*-dimethylaminoethyl methacrylate), PDMAEMA, and poly(acrylic acid), PAA. The dynamics of making and breaking ionic bonds between the oppositely charged chains underlie

all linear viscoelastic properties of the complex coacervates. We treat (clusters of) ionic bonds as sticky points and find that there is a remarkable resemblance between the relaxation spectra of these complex coacervates and the classical sticky Rouse model for single polymer systems. Salt affects all relaxation processes in the same way, giving rise to a widely applicable time–salt superposition principle. The viscoelastic properties of the complexes are very different from those of the individual components. In the complexes with a chain length mismatch, the effect of the mismatch on the viscoelastic properties is not trivial: changing the length of the polycation affects the relaxation behavior differently from changing the length of the polyanion.



■ INTRODUCTION

Complexation between oppositely charged macromolecules can lead to a variety of structures and materials with diverse properties. By choosing the right size and charge of the macromolecules, this complexation can be used to drive the formation of, for example, membranes,¹ vesicles,² spherical and wormlike micelles,³ fibers,⁴ and soft gels.⁵ Various natural materials rely on the same interactions for their formation. Many bioadhesives contain a significant fraction of oppositely charged residues and behave much like polyelectrolyte complexes.^{6,7} Similarly, chromatin fibers are formed when histon proteins condense strands of DNA⁸ and blood clotting factors are anchored to cell membranes near an injury with the help of an electrostatic complex of phospholipids and the calcium-rich GLA domain of clotting proteins.⁹ In all these cases the properties of the complexes or materials are governed by the dynamics of the ionic bonds that are created between the oppositely charged species. Many parameters, such as salt concentration and size of the charged macroions, affect the strength and relaxation dynamics of ionic bonds significantly, in a way we understand qualitatively.^{5,7,10} However, a quantitative understanding of the effect of salt, the size, and charge of the interacting macromolecules and cooperativity of the ionic bonds between them on the relaxation dynamics of electrostatic complexes is still lacking.

In this paper, we use rheology to study the relaxation dynamics in polyelectrolyte complex coacervates of different composition and chain lengths and at varying salt concentration. Complexes of oppositely charged homopolyelectrolytes offer a well-defined model system to study the processes that

occur locally in many of the charge-driven materials mentioned above. The complexation between oppositely charged polyelectrolytes in solution leads to a macroscopic phase separation at the right mixing ratio and below a critical salt concentration.^{10,11} The complex coacervate phase is held together by thermodynamically favorable interactions between the oppositely charged polyelectrolyte chains, which may be partly enthalpic, partly entropic in nature.¹² We vary the chain length of both polymers independently to investigate if groups of multiple subsequent ion pairs form along the chains and how the cooperativity of these domains influences the rheological behavior. We find that the ionic bonds are essentially temporary cross-links that are labile at long enough time scales and can be treated as effective friction points in our rheological characterization. Salt is a plasticizer for these cross-links and affects all relaxation processes in the same way.¹³ This gives rise to a generic relaxation time spectrum for polyelectrolyte complexes and for ionic bonds, which should be applicable in other charge-driven materials as well.

Previous reports on the rheology of polyelectrolyte complexes mostly focus on soluble complexes in aqueous solution because of their potential application as capsules.^{14,15} These complexes are typically formed at very low salt concentrations and a mixing ratio far outside the region where associative phase separation takes place. Dilute solutions of soluble complexes have a slightly increased zero shear

Received: August 16, 2012

Revised: February 3, 2013

Published: February 14, 2013



viscosity compared to solutions with only one type of polymer and show moderate shear thinning behavior at very high shear rates.^{14,15} In concentrated polyelectrolyte solutions, well above the entanglement concentration, addition of small amounts of an oppositely charged polyelectrolytes leads to a more pronounced increase in viscosity and in both shear moduli, but the underlying relaxation mechanisms remain unclear.¹⁶ On the other hand, in three studies on phase-separated complex coacervates of proteins and flexible polymers molecular models for the complexes have been proposed based on the rheological measurements. In all models, the proteins form junction points in a network of flexible polyelectrolytes.^{17–19} The strength of the junction points varies from weak and reversible^{17,18} to nearly permanent,¹⁹ depending on the type and charge density of the protein and the salt concentration in solution.

When complexes are formed between two flexible polyelectrolytes, the structure of the complex might be significantly different from the structure of a protein–polyelectrolyte complex.^{17–19} Junction points between two flexible polyelectrolytes can span a much wider range of sizes, and they may become much tighter due to the high charge density of some polyelectrolytes. In order to obtain insight into the dynamic properties of these flexible complex networks, we study linear rheology of a model polyelectrolyte complex coacervate of two flexible polyelectrolytes. We focus on the effect of salt, polymer chain length, chain length matching, and mixing stoichiometry.

MATERIALS AND METHODS

We use two oppositely charged flexible polyelectrolytes with pH-dependent charges to form the polyelectrolyte complex coacervates for our rheological investigation. As a polyanion we use poly(acrylic acid), PAA, with five different chain lengths (N_{an}): 20 ($M_n = 1.5$ kg/mol, $M_w/M_n = 1.2$), 47 ($M_n = 3.4$ kg/mol, $M_w/M_n = 1.30$), 139 ($M_n = 10.0$ kg/mol, $M_w/M_n = 1.15$), 500 ($M_n = 36.0$ kg/mol, $M_w/M_n = 1.10$), and 1730 ($M_n = 124.5$ kg/mol, $M_w/M_n = 1.25$). As a polycation we use poly(*N,N*-dimethylaminoethyl methacrylate), PDMAEMA, with four different chain lengths (N_{cat}): 17 ($M_n = 2.7$ kg/mol, $M_w/M_n = 1.18$), 51 ($M_n = 8.0$ kg/mol, $M_w/M_n = 1.40$), 150 ($M_n = 23.5$ kg/mol, $M_w/M_n = 1.04$), and 527 ($M_n = 82.7$ kg/mol, $M_w/M_n = 1.09$). All polymers are purchased from Polymer Source, except for $N_{an} = 20$, which is purchased from Sigma-Aldrich. We prepare stock solutions of all polymers at 30 g/L (PAA) or 50 g/L (PDMAEMA) in Milli-Q water with the pH adjusted to 6.5 ± 0.2 using 1.0 M HCl and KOH. At this pH both polymers have equal charge densities ($\alpha_+ = \alpha_- = 0.95$) at salt concentrations between 0.10 and 1.0 M (see Supporting Information).

Polyelectrolyte complex coacervates are prepared by mixing PAA and PDMAEMA at a 1:1 molar ratio of chargeable groups unless stated otherwise. We adjust the overall salt concentration using a 3.0 M KCl stock solution and correct for the counterions present in the polymer stock solutions. In all cases we prepare a total volume of 4 mL with an overall polymer concentration of 0.20 M, measured in monomer units. A detailed report of the process of complexation is given elsewhere.¹¹ We check that the pH after complexation in both the dilute and the complex coacervate phase is equal to the original pH of the stock solutions within experimental error (see Supporting Information).

For rheological measurements we leave all samples to equilibrate for at least four days. One or two days after mixing we centrifuge the samples at 3000g for 5–10 min to ensure that all droplets of the dense complex coacervate phase are collected at the bottom of our sample tubes. After the total equilibration time, we separate the top dilute phase from the bottom complex coacervate phase (see Figure 1 for an example) and directly load the complex coacervate phase onto the cone–plate geometry of the rheometer.

The rheological measurements are carried out on Anton Paar MCR301 and MCR501 series stress-controlled rheometers using a cone–plate geometry with a cone radius of 25 mm and a cone angle of



Figure 1. Coexistence between a complex coacervate phase and a dilute phase in a mixture of PAA₁₃₉ and PDMAEMA₁₅₀ at 1.0 M salt. 20% fluorescently labeled PAA₁₃₉ was added to enhance the distinctness of the separated phases.

1°. We keep the temperature controlled at 20 °C with Peltier elements, and we use an evaporation blocker to minimize water evaporation. With every sample, we perform a series of measurements, all separated by a waiting step that is at least 5 times longer than the apparent longest relaxation time we find in a step-strain experiment. However, we make sure that the total duration of a measurement series never exceeds 5 h to ensure that the slow solvent evaporation that occurs despite our use of an evaporation blocker has a negligible effect on the rheological measurements (see Supporting Information).

We study the relaxation behavior of these complex coacervates by both step-strain and frequency-sweep experiments to cover a range of time scales from milliseconds (frequency sweep) to hours (step strain). In all cases we apply a maximum deformation that is still in the linear viscoelastic regime, which extends to deformations of 100%, typical for polymeric materials, and is only weakly dependent on salt concentration (see Supporting Information).

From the step-strain and frequency-sweep measurements, we calculate relaxation spectra $H(\tau)$ by approximating the relaxing complex coacervates as a sum of Maxwell elements

$$G(t) = \sum_{i=1}^M G_i e^{-t/\tau_i} \quad (1)$$

$$G'(\omega) = \sum_{i=1}^M \frac{G_i \omega^2 \tau_i^2}{1 + \omega^2 \tau_i^2} \quad (2)$$

$$G''(\omega) = \sum_{i=1}^M \frac{G_i \omega \tau_i}{1 + \omega^2 \tau_i^2} \quad (3)$$

where the M relaxation modes, defined by their relaxation strength G_i and their relaxation time τ_i , are taken equally spaced on a logarithmic scale.²⁰ The corresponding relaxation spectra $H(\tau)$ of the complex coacervates are obtained by iterative fitting of both the relaxation modulus $\log G(t)$ and the storage $\log G'(\omega)$ and loss modulus $\log G''(\omega)$, using a least-squares approximation, and are defined by^{21,22}

$$H(\tau) = \sum_{i=1}^M G_i \delta\left(1 - \frac{t}{\tau_i}\right) \quad (4)$$

where $\delta(x)$ denotes the Dirac delta function. The advantage of using this combination of relaxation modulus and frequency-sweep data is that they can be directly converted into relaxation spectra. We confirm that our fitting yields relaxation spectra that are indeed characteristic for the complex coacervates we study in two ways.

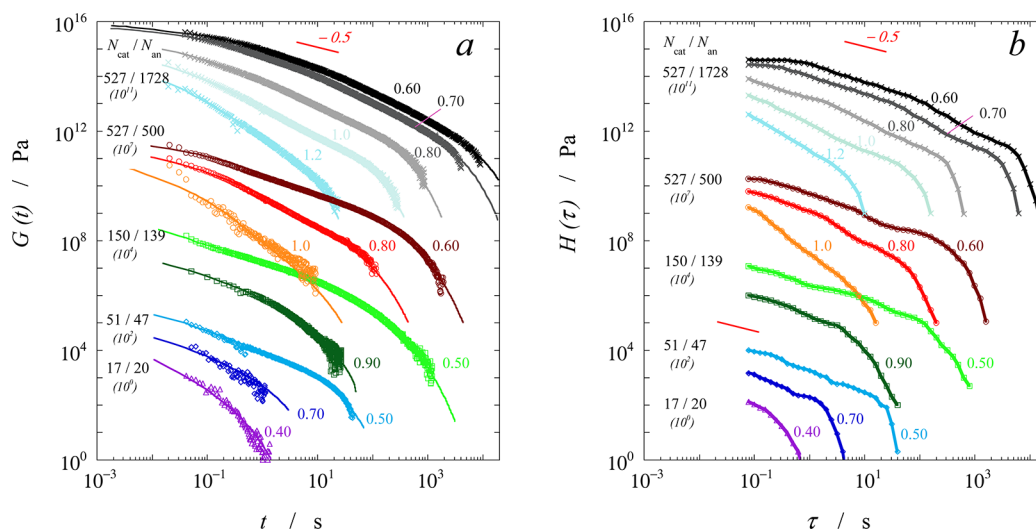


Figure 2. (a) Stress relaxation modulus of PDMAEMA/PAA complex coacervates at different salt concentrations and for different polymer chain lengths. In all cases a step strain of 10–20% is applied. (b) Logarithmic relaxation time spectra of the same samples. The labels to the left of the curves ($N_{\text{cat}}/N_{\text{an}}$) indicate the chain length of the polycation and the polyanion, respectively. All curves are shifted vertically for clarity using the shift factor that is shown in parentheses at the left of the curves. The numbers at the right indicate overall salt concentrations (KCl, in M).

First of all, we verify that the feedback loop in the stress-controlled rheometer allows carrying out the step-strain measurements with sufficient accuracy, by converting our step-strain measurements $G(t)$ into creep functions $J(t)$, using the numerical Hopkins–Hamming method for the convolution integral of the relaxation modulus and creep compliance (see Supporting Information).²³ As a complementary verification, we convert independently measured creep curves $J(t)$ into relaxation moduli following a two-step approach, as discussed in the Supporting Information.^{24,25} The good agreement we find between both converted and experimentally measured relaxation moduli and creep compliances supports our assumption that the relaxation spectra of these complex coacervates can be obtained from the relaxation moduli, using the approach described above.

Second, we compare the fitted relaxation spectra to the relaxation spectra obtained directly from the storage and loss moduli using the approximate relation between the relaxation spectrum and the local derivative of the storage or loss modulus of Williams and Ferry (see Supporting Information).²⁵ This comparison confirms that the fitting procedure described above yields reproducible relaxation spectra.

RESULTS AND DISCUSSION

Relaxation Dynamics in Matched Complexes. The phase behavior of complex coacervates of PAA and PDMAEMA depends both on salt concentration and on chain length, as complex coacervates are formed as one of the phases at binodal composition in the associative phase separation of solutions of oppositely charged polymers.¹¹ The polymer volume fraction inside the complexes varies between 0.05 and 0.30 (effective concentration of monomeric units $c_p = 0.5$ –3 M), whereas the overlap concentration varies between $c_p = 0.01$ and 0.1 M, depending on the chain length ($N = 1728$ –20, assuming random walk statistics). By analogy with ordinary polymer solutions, these complexes are typically in a concentration range between semidilute and concentrated. However, because of the sometimes strong interactions between the two polymeric components, their rheological behavior is very different from solutions of the individual polymers at the same concentration (see Supporting Information).

Figure 2a shows the relaxation moduli of complex coacervates in which the polycation length is matched closely

to the polyanion length ($0.85 < N_{\text{cat}}/N_{\text{an}} < 1.1$) and one for which the polyanion is significantly longer than the polycation ($N_{\text{cat}}/N_{\text{an}} = 527/1728$). The salt concentration is varied from a lower limit of 0.40 M, below which equilibration of the complex coacervate samples is experimentally not feasible, to an upper limit close to the critical salt concentration, above which the mixed polymer solutions no longer phase separate into a dilute phase and a complex coacervate phase.¹¹ Curves corresponding to the same combination of chain lengths are shifted vertically using the same prefactor for clarity.

At all time scales up to the terminal relaxation time, we clearly find a continuous decrease of the relaxation modulus in all curves, indicating that relaxation processes occur on all time scales between tens of milliseconds and the terminal relaxation time, which increases with increasing chain length and decreasing salt concentration. Neither chain length nor salt concentration has a strong effect on the shape of the relaxation curve in between the terminal relaxation time and the inertial lower limit. In fact, all curves seem to exhibit a regime with a constant slope α , between -0.5 and -0.7 , in which the modulus scales as $G(t) \sim (t/\tau)^\alpha$. At short times, this regime is bound by a leveling off to a presumed plateau, for the lowest salt concentrations and longest chain lengths.

The relaxation spectra corresponding to these step-strain experiments show the same characteristics (see Figure 2b). In our approach, these relaxation spectra are limited at low τ to several milliseconds by the highest measured frequency where inertia is still negligible in a frequency-sweep experiment and at high τ by the terminal relaxation time.

In polymer solutions, such a regime with constant slope is characteristic for Rouse or Zimm dynamics of the polymer chains. On the basis of the composition of these complex coacervates, which contain up to 70 wt % water, we expect hydrodynamic interactions between the monomers.¹¹ At the same time, the polymer concentration in the complex coacervates is rather high, and hydrodynamic interactions are screened by segments of other polymer chains at a typical hydrodynamic screening length ξ_h , which is approximately equal to the static correlation length.²⁶ At short length scales, we thus expect Zimm relaxation modes, including hydro-

dynamic interactions to govern the polymer dynamics. At larger length scales, we expect the polymer dynamics to be governed by Rouse modes. Such relaxation behavior indeed gives rise to a constant slope of both $\log G(t)$ versus $\log t$ and $\log H(\tau)$ versus $\log \tau$, which is -0.5 for ideal chains in the Rouse model (-0.46 in good solvent), and -0.67 for ideal chains in the Zimm model (-0.57 in good solvent). The relaxation moduli and relaxation spectra in Figure 2 exhibit regimes with a slope close to -0.5 , in agreement with the expected Rouse modes at length scales beyond the hydrodynamic screening length. We note that we do not see clear signs of entanglements in these complex coacervates. Such entanglements are expected to show as plateau in the relaxation modulus, and, in addition, the typical crossover moduli (see hereafter in Figure 5b) would be significantly higher.²⁵

Molecular Relaxation Model for Matched Complexes.

Our observation of Rouse-like relaxation at time scales up to 1000 s is, at first sight, rather surprising. The typical time scales where classical Rouse (or Zimm) dynamics are observed for ordinary polymer chains of similar length is orders of magnitude lower than the time scales where we observe Rouse-like dynamics.^{25,27} What relaxation mechanism could underlie these slow Rouse modes?

In a polyelectrolyte complex, ionic bonds form reversible bonds between oppositely charged polyelectrolyte chains. These bonds act as “sticky” points that enhance the effective friction of polymer chains and slow down their mobility.²⁸ Since stress relaxation in these polymeric systems occurs by movement of chains, we expect ionic bonds to slow down the stress relaxation. The average time these ionic bonds keep two oppositely charged segments together can be approximated as^{13,28}

$$\tau_0 = \frac{1}{\omega_0} \exp\left(\frac{E_a(c_{\text{salt}})}{k_B T}\right) \quad (5)$$

where ω_0 is the relaxation rate in the absence of ionic bonds and where E_a represents the energy difference between the bound and unbound oppositely charged segments.¹³ Following our previous work, we estimate the energy barrier from the rearrangement process of two ion pairs. When bound, we approximate the energy of the ionic bonds by an effective Coulomb energy. When the ionic bonds rearrange, they go through an unbound state where the four ionic groups are surrounded by electrolyte, for which we use a Debye–Hückel approximation. Combining these two terms, we get

$$\frac{E_a}{k_B T} = -2\kappa l_B + \frac{2l_B}{d} = -A\sqrt{c_{\text{salt}}} + B \quad (6)$$

where $l_B = e^2/4\pi\epsilon_r\epsilon_0 k_B T$ is the Bjerrum length and d is the effective contact distance of an ionic bond. The constant $A = (32 \times 10^3 \pi N_A l_B^3)^{1/2}$ and $B = 2l_B/d$. The factor 2 accounts for the fact that rearrangements involve two ion pairs that exchange their partners. We note that the Debye–Hückel approximation assumes that ions are point charges in a continuum dielectric, whereas we use high salt concentrations to study the rupture of ionic bonds, where these assumptions may not be entirely valid. Moreover, the connectivity of the charges along the polyelectrolyte chains is not taken into account here because our model describes only the local rearrangement of ionic bonds. Nonetheless, we have previously found that this simple expression adequately describes the effect of competition between monovalent salt ions and polymeric charges in

complexes between oppositely charged polyelectrolytes, and we therefore apply it here as well.¹³

In the complexes studied here the sticky points are present along the entire polymer chain. Consequently, broken bonds may easily re-form with new partners and renormalization of bond lifetimes may be neglected.²⁸ Moreover, when geometric positioning of the groups allows, several subsequent segments of a polymer chain may bind to another polymer chain to form sticky clusters with multiple ionic bonds. These cooperative bonds should have a proportionally higher bond energy, when no external force is applied to the bonds.²⁹ We will see hereafter that these higher energy barriers seem not to play a role in the rheological behavior of complex coacervates.

According to the model of sticky polymer dynamics, the stress relaxation modulus decays as a power-law at time scales much larger than for nonsticky polymers (Rouse or Zimm). For example, the sticky Rouse modes are given by

$$\tau_p \approx \tau_0 \left(\frac{f}{p}\right)^2 \quad 1 < p < f, \quad \tau_R = \tau_0 f^2 \quad (7)$$

where f is the number of ionic bonds per chain and τ_0 is given by eq 5. At short times ($p \approx f$), only small parts of the polymer chain are mobile and part of the stress can relax. As time progresses, more and more ionic bonds break and re-form in different places and larger parts of the polymer chain become mobile. Finally, after some terminal relaxation time τ_R ($p = 1$, see Supporting Information), determined by the chain length and the salt concentration, the whole polymer chain can move and all stress can be relaxed. After the terminal relaxation time, we therefore expect an exponentially decreasing stress, as is observed in the relaxation curves in Figure 2a for most complex coacervates.

The modulus level at the terminal relaxation time is roughly $k_B T$ per chain: $G(\tau_R) \approx k_B T \phi_p / N b^3$. The modulus at the elementary lifetime of a single sticky point τ_0 is approximately $k_B T$ per sticky point.

An important consequence of eqs 5 and 6 is that salt affects all sticky modes in the same way. In other words, salt can be used as a plasticizer for the ionic bonds to access a different part of the relaxation spectrum of polyelectrolyte complexes.¹³ Indeed, the relaxation time spectra at different salt concentrations in Figure 2b can be rescaled by shifting along the τ -axis to obtain a relaxation spectrum master curve (see Figure 3). The same holds for frequency sweeps measured at different salt concentrations. Figure 4 shows how this leads to a single frequency sweep master curve for each chain length. The insets in Figure 4 show the relaxation spectra that were used to fit these curves. These spectra show all characteristics of the relaxation spectra in Figure 2b.

The shift factors $\tau_c \propto \tau_0$ (eq 5) and G_c (see Figure 5 and Supporting Information) provide a way to compare the relaxation times and the moduli of the complex coacervates at different salt concentrations. We choose the reference condition for all shift factors such that the crossover between G' and G'' , extrapolated from the low-frequency viscous limit in the frequency sweeps (Figure 4), occurs at a rescaled frequency $\omega \tau_c = 1$ and a rescaled modulus $G'/G_c = 1$.

The τ_c can be fitted using eqs 5 and 6, with a value of A that corresponds to rearrangements of single ionic bonds, in pairs as described above, in an aqueous solution of high ionic strength (for $T = 293$ K and $\epsilon_r = 44$, $A = 12$).³⁰ The value of B cannot be fitted independently from the exponential prefactors in eqs 5

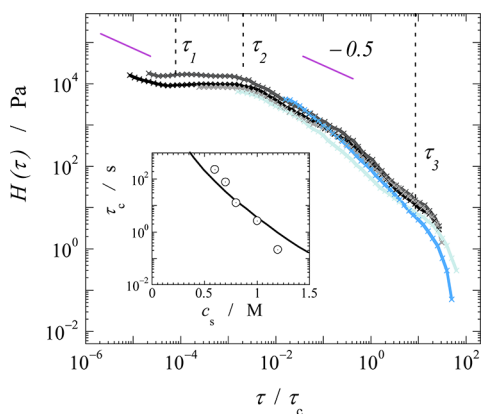


Figure 3. Rescaled logarithmic relaxation time spectra of the $N_{\text{cat}}/N_{\text{an}} = 527/1728$ complex coacervates at different salt concentrations. The inset shows the time scaling factors τ_c as a function of salt concentration, with a fit to eqs 5 and 6.

and 6. For G_c we find a much weaker dependence on salt concentration. The typical complex coacervate modulus seems to decrease with increasing salt concentration (see Figure 5b) because the binodal polymer concentration, and hence the density of sticky points, also decreases with increasing salt concentration in these associatively phase separating systems.¹¹

In the relaxation spectra in Figures 2b and Figure 3 three regimes can be distinguished. At intermediate time scales ($\tau_2 < t < \tau_3$), we find a regime of Rouse-like stress relaxation, as discussed above. Just before the terminal relaxation time τ_3 the relaxation spectra fall off more rapidly than in the intermediate regime, most likely because all single ionic bonds have fully relaxed and only clusters of multiple bonds still contribute to the modulus.

At short time scales we observe a plateau ($\tau_1 < t < \tau_2$) and subsequent upturn ($t < \tau_1$) in the relaxation spectra of the longest polymer chains. Intuitively, we would attribute the onset of this plateau (τ_2) to the elementary lifetime of a single sticky point τ_0 (see eq 5). Based on the relaxation spectrum in Figure 3 and the corresponding shift factors τ_c , the lifetime of a single ionic bond would be 200 ms at 0.6 M, which is of the same order of magnitude as the unperturbed ionic bond lifetimes we previously found in single molecule force spectroscopy measurements.²⁹ From the modulus level at this single ionic bond lifetime $G(\tau_0) \approx k_B T \phi_p / b^3$ and the modulus level at the apparent terminal relaxation time $G(\tau_R) \approx k_B T \phi_p f / N b^3$ (see Supporting Information), we estimate the number of ionic bonds per chain to be 10^2 – 10^3 for the PDMAEMA₅₂₇/PAA₅₀₀ complex coacervates, which is quite reasonable for these chain lengths ($N_{\text{cat}} = 527$, $N_{\text{an}} = 500$).

The presence of a plateau ($\tau_1 < t < \tau_2$) suggests that relaxation processes still take place at time scales shorter than the lifetime of a single ionic bond, which can also be seen from the fact that the relaxation modulus at the lowest salt concentrations in Figure 2a is still continuously decreasing with increasing time. At time scales $t < \tau_1$, we even observe an increased relaxation in the high-frequency region of some of the frequency sweeps at these low salt concentrations (see Figure 4). Possibly, this relaxation at time scales shorter than the elementary lifetime of the ionic bonds originates from Rouse modes of not fully complexed chains in regions within the sample where the density of polymer chains is slightly lower.¹⁷ Alternatively, these modes might originate from ionic bonds that are less tightly bound due to local steric or conformational

hindrance. On the basis of the time scales where we find the increased relaxation, $O(10 \text{ ms})$, and the estimated number of ionic bonds per chain, we believe these relaxation processes are unlikely to originate from “classical” Rouse or Zimm modes of the chains segments between associations.

Viscosity of Polyelectrolyte Complex Coacervates.

The sticky polymer dynamics model for polyelectrolyte complex coacervates as presented above not only provides an accurate description of the relaxation mechanisms occurring in the complexes but also gives a prediction for the zero-shear viscosity as a function of salt concentration, polymer concentration, and, at least theoretically, polymer chain length. The zero shear viscosity is proportional to the terminal relaxation time in the sticky polymer dynamics model, τ_R , and modulus at this terminal relaxation time, which is $k_B T$ per chain.²⁸

$$\eta_0 \approx \frac{k_B T \phi_p \tau_R}{b^3 N} \propto N^{\beta_1} \phi_p(N, c_{\text{salt}})^{\beta_2} \exp(-A\sqrt{c_{\text{salt}}} + B) \quad (8)$$

where b is the Kuhn length and $\phi_p/b^3 N$ is the number density of chains. In the sticky polymer dynamics model, the terminal relaxation time for ideal chains scales with $\tau_0 N^2$ (eq 5; in good solvent the exponent is 2.18), assuming hydrodynamic interactions are screened at the size of the chains, and β_1 is unity (1.18 in good solvent).²⁸

Figure 6 shows the zero-shear viscosity of the polyelectrolyte complex coacervates as a function of salt concentration and chain length. Equation 8 predicts a stretched exponential dependence of the viscosity on the salt concentration, as ϕ_p depends only weakly on salt concentration.^{11,13} We find good agreement of our data with a stretched exponential fit for all chain lengths, using the same parameters A and B , as in Figure 5. Close to the critical salt concentration (indicated with arrows) the model breaks down, and the viscosity decreases more rapidly than predicted.

The parameter A takes the value of 12 in both Figure 5a and Figure 6, which is in close agreement with the expected value for the rearrangement of single ionic bonds in a solution at $T = 293 \text{ K}$ with an effective dielectric constant of $\epsilon_r = 44$, that is, the dielectric constant for a 2–3 M total ionic strength solution.³⁰ Interestingly, the presence of clusters of ionic bonds, for which the energy barrier for dissociation should be significantly higher, does not affect the value of A , which represents the relevant energy barrier for stress relaxation. Apparently, stress relaxation of clusters of ionic bonds proceeds via small steps of single rearrangements with an energy barrier equal to eq 6, similar to trains of multiple polymer segments that are adsorbed to a surface, where the relevant energy barrier governing the lateral mobility of chains on the surface is also the adsorption energy of a single segment.^{31–33}

The predicted dependence of the viscosity on the polymer chain length (eq 8) is not trivial because these complex coacervates form by associative phase separation and the coacervate phases studied here correspond to the composition at the binodal (see Figure 1). The thermodynamic driving forces of this process are affected by both polymer chain length and salt concentration. From experiments, we know that the binodal polymer concentration ϕ_p increases moderately with increasing chain length and more strongly with decreasing salt concentration.¹¹ In the original sticky polymer dynamics model, α is close to unity.²⁸ However, the assumptions that the typical

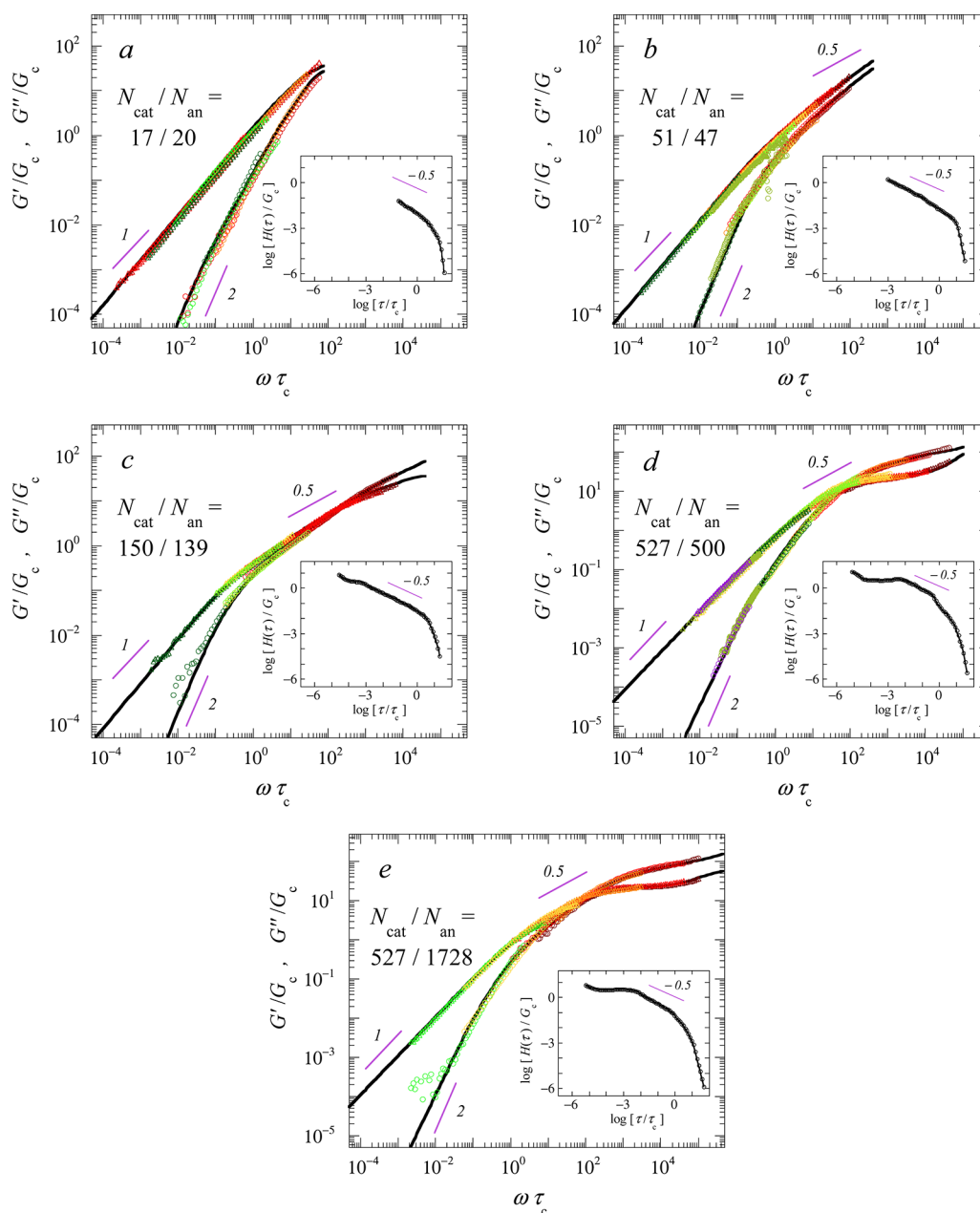


Figure 4. (a–e) Rescaled frequency sweeps of PDMAEMA/PAA complex coacervates of different polymer chain lengths, $N_{\text{cat}}/N_{\text{an}} = 17/21$ (a), 51/47 (b), 150/139 (c), 527/500 (d), and 527/1728 (e). The frequencies have been rescaled using salt-dependent shift factors τ_c , storage and loss moduli using salt-dependent shift factors G_c (see Figure 5), taking the crossover between G'/G_c and G''/G_c , extrapolated from the low-frequency viscous limit, at $\omega\tau_c = 1$ and $G'/G_c = 1$ as reference condition. In all frequency sweeps a strain amplitude of 5% or less was applied. The insets show the logarithmic relaxation time spectra that are used to fit the rescaled frequency sweeps. Where appropriate, approximate slopes have been indicated using their power law exponent. (f) Example logarithmic relaxation time spectrum of a 527/1728 complex coacervate at 0.60 M salt, showing three regimes (τ_1 – τ_3).

distance between subsequent sticky points is independent of chain length and that the polymer volume fraction can be fixed at the same value for all chain lengths probably do not hold for complex coacervates. Especially the polymer volume fraction is systematically higher for longer polymer chains at the same salt concentration, as the translational entropy and, hence, their tendency to oppose concentration in the condensed complex coacervate is smaller for long polymer chains.¹¹ Given the fact that the viscosity in the sticky polymer dynamics models depends very strongly on the polymer concentration, we expect a significant deviation from the classical slope of unity for complex coacervates. Experimentally, we find a power law

dependence, with slopes decreasing with salt concentration from 2.3 at 0.50 M salt to 1.2 at 1.0 M salt (see Figure 6b).

In analogy with Figure 6a, there is a critical chain length, below which no complexation occurs at a given salt concentration. The existence of a critical chain length in complex coacervates at a fixed salt concentration has been observed before and is predicted to be more general.³⁴

Finally, we can estimate the terminal relaxation time τ_R from Figure 2b. We find that these terminal relaxation times show a similar power law dependence on chain length (see Figure 7). Here, the dependence is no longer affected by the N dependence of ϕ_p , and we find a power law slope of 2 ± 0.3 ,

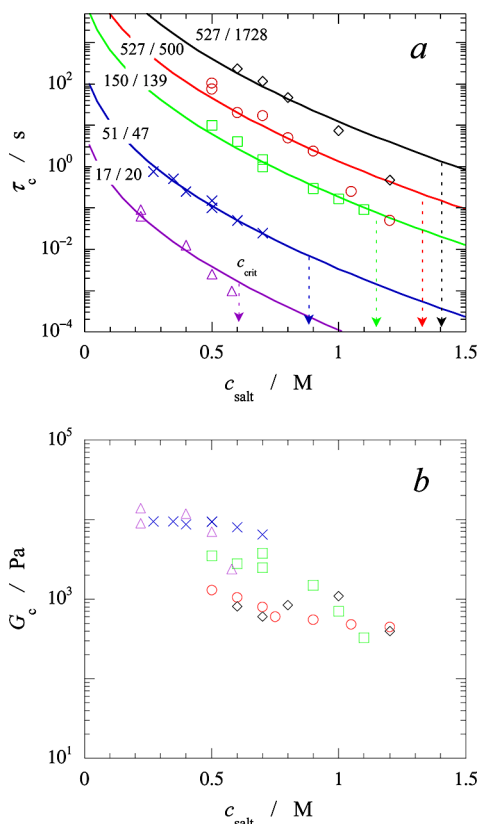


Figure 5. (a) Relaxation times and (b) moduli shift factors for the frequency-sweep data shown in Figure 4. Symbols indicate complex coacervates of different chain lengths, as indicated in (a). The solid lines in (a) are fits to eqs 5 and 6. The vertical dashed arrows in (a) indicate the critical salt concentrations for each chain length combination.

in agreement with the slope of 2 predicted by the sticky polymer dynamics model.

Nonstoichiometric Complex Coacervates. When polycations and polyanions are mixed in a nonstoichiometric ratio, complex coacervates may still form.^{12,18,19} In some cases, the rheological properties of the complex coacervates depend strongly on the mixing ratio.¹⁹ In other cases, no dependence or a much weaker dependence is found.^{15,18} The degree of charging of the polyelectrolytes may play an important role in explaining this difference.¹² In addition, if the complex coacervates have a preferred composition, then excess polycation or polyanion mainly ends up in the dilute phase, thereby leaving the rheological properties of the complex almost unchanged. By contrast, if the composition of the complex coacervates changes notably with a changing mixing ratio of polycation and polyanion, then its rheological properties may also change significantly.

In order to investigate the effect of mixing stoichiometry on the relaxation behavior of PDMAEMA/PAA complex coacervates, we have prepared complex coacervates of two flexible polyelectrolytes ($N_{\text{cat}} = 527$ and $N_{\text{an}} = 500$) at different overall mixing ratios. For each sample we perform a frequency sweep, creep test, and flow curve. We use the dilute phase of each sample to establish whether excess of one of the polymers is present in the dilute phase by adding a solution of either polycation or polyanion and checking for complexation by eye. For these polyelectrolytes we find that, irrespective of the initial mixing stoichiometry, the complex coacervates acquire a fixed

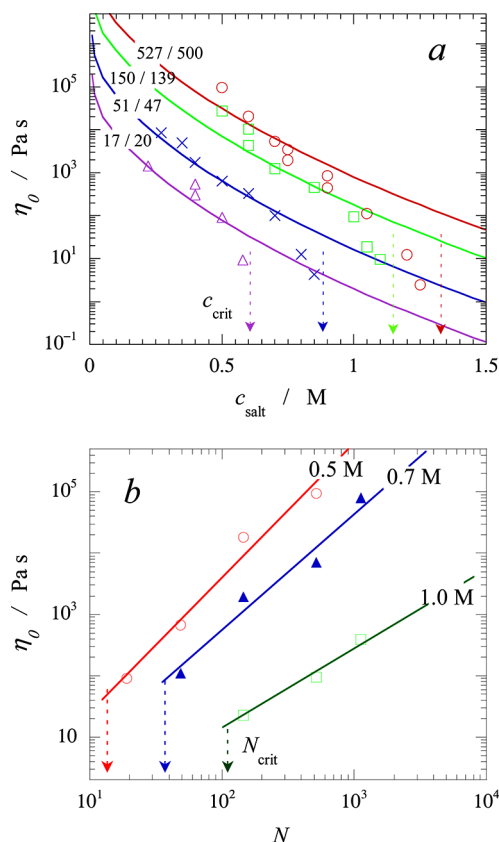


Figure 6. (a) Zero shear viscosity as a function of overall salt concentration for PDMAEMA/PAA complex coacervates of different polymer chain length. Solid lines are fits to eq 8. (b) Zero shear viscosity as a function of average polymer chain length in the complex coacervate for different salt concentrations. Solid lines are power law fits to the data. Vertical dashed arrows indicate (a) critical salt concentration above which or (b) critical chain lengths below which we no longer find complexation.

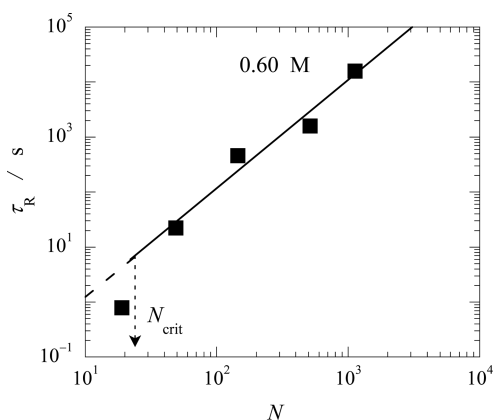


Figure 7. Terminal relaxation time (τ_R) from Figure 2a as a function of the average polymer chain length (N_{cat} and N_{an}) in the complex coacervate for a salt concentration of 0.60 M. The terminal relaxation time for $N_{\text{cat}}/N_{\text{an}} = 51/47$ and 150/139 are estimated by interpolation between the salt concentrations depicted in Figure 2a using eqs 5 and 6. For $N_{\text{cat}}/N_{\text{an}} = 17/20$ the terminal relaxation time for 0.40 M salt is shown, as 0.60 M is above the critical salt concentration for this chain length. The solid line is a power law fit to all chain lengths above 40, and has a slope of 2.0 ± 0.3 .

composition of $f^+ = 0.47 \pm 0.06$ (based on monomer units). This composition is close to the 1:1 stoichiometric charge ratio ($f^+ = 0.5$) that is typically found for polyelectrolyte complexes in micelles,³⁵ in soft gels³⁶ and in bulk.³⁷

Figure 8 shows the storage and loss moduli of the complexes at $\omega = 1$ rad/s and the zero-shear viscosity as a function of the

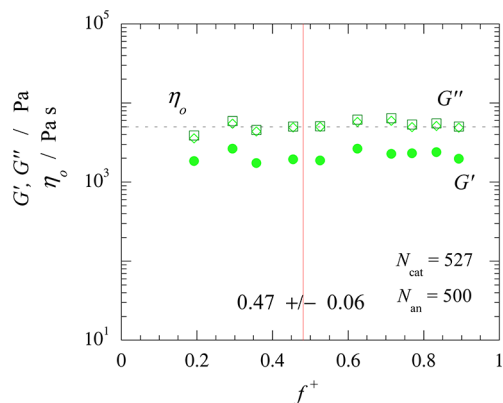


Figure 8. Linear viscoelastic properties of PDMAEMA₅₂₇/PAA₅₀₀ complex coacervates as a function of the overall stoichiometry f^+ , defined as the molar ratio of positive chargeable monomeric units to total chargeable monomeric units. The horizontal line indicates the average zero shear viscosity for all compositions. The vertical line indicates the average stoichiometry of the complex coacervate phase that was formed. Storage and loss moduli are determined at an angular frequency of 1.0 rad/s.

fraction of positively charged monomers in the overall mixture (full frequency sweeps in Supporting Information). As expected, we find no significant difference between the samples. Excess polycation or polyanion ends up in the dilute phase and the complex coacervate phase maintains a more or less constant, “preferred” composition.¹²

Complex Coacervates with Unmatched Chain Lengths. Polycations and polyanions of unequal length can form complex coacervates as well. The length asymmetry of the polymers may have a pronounced effect on the rheological behavior.^{15,17} In Figure 9, we show the effect of chain length mismatch on the rheological behavior of complex coacervates of these flexible polyelectrolytes. We find that there is an asymmetry between changing the length of the polycation and changing the length of the polyanion.

When we decrease the length of PDMAEMA and leave the length of PAA unchanged for $N_{an} = 500$, the viscoelastic response changes significantly. Both storage and loss modulus are slightly lowered, as a result of the slightly lower polymer volume fraction in the complex coacervates with shorter chains.¹¹ More importantly, the crossover point shifts to much higher frequencies when the PDMAEMA length is decreased, indicating that the long-time sticky Rouse modes, corresponding to long parts of a polymer chains, vanish, and only the short-time modes, corresponding to small segments or small chains, remain.

By contrast, when we decrease the length of the PAA, while leaving PDMAEMA unchanged, we find that the linear viscoelastic response of the complex remains almost unchanged for $N_{cat} = 527$ ($N_{an} = 500, 139, 47$) and $N_{cat} = 150$ ($N_{an} = 139, 47$). When the PAA becomes too short ($N_{an} = 20$), the viscoelastic response seems to change slightly and the crossover shifts to higher frequencies.

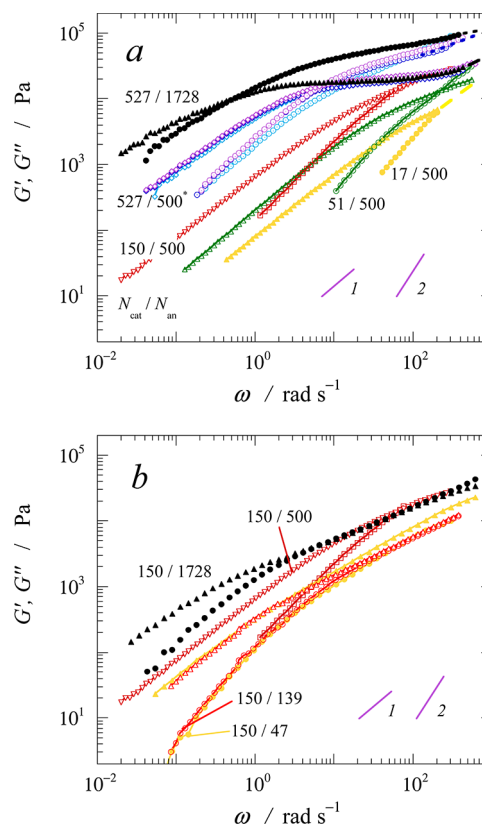


Figure 9. Frequency sweeps of PDMAEMA/PAA complex coacervates with unmatched chain lengths, as indicated by the labels (N_{cat}/N_{an}), at 0.70 M salt and $f^+ = 0.5$. In all cases a strain amplitude of 5% was applied. The frequency sweeps of complex coacervates with chain lengths 527/500, 527/139, 527/47, and 527/20 overlap to a large extent. For reasons of clarity we show only the label for 527/500, marked with an asterisk.

However, when we increase the length of the PAA, we do find significant change in the viscoelastic response and the apparent crossover point, extrapolated from the viscous regime, shifts to lower frequencies for $N_{cat} = 527$ ($N_{an} = 1728$) and $N_{cat} = 150$ ($N_{an} = 500, 1728$). Instead of PDMAEMA, PAA now seems to dictate the rheological behavior.

These results indicate that, although the polymers are present in a 1:1 ratio of chargeable groups, they do not have the same effect on the sticky network of overlapping polymer chains. It seems that mainly PDMAEMA governs the relaxation behavior, as decreasing the PAA length does not affect the linear viscoelastic response of the complex coacervates. We speculate that the PAA chains may play a similar role as the negatively charged BSA in PDADMAC/BSA complex coacervates,¹⁷ acting only as sticky temporary cross-links in a PDMAEMA-dominated network. Only when the PAA chains become much longer than the PDMAEMA chains, they start affecting the linear viscoelastic response because the PAA chains start overlapping. However, this picture is highly speculative, and additional structural information on these complex coacervates is needed to better understand the role of both the polycations and the polyanions in the dynamics and the mechanical properties of these complex coacervates.

CONCLUSIONS

We find that the rheological behavior of polyelectrolyte complexes composed of flexible polyelectrolytes is dominated

by the dynamics of the single ionic bonds between the polyelectrolyte chains. This mechanism is in line with the suggested network structure of PDADMAC/BSA complex coacervates.¹⁷ The ionic bonds act as temporary cross-links, and their dynamic formation and rupture can be influenced by adding salt. Relaxation of stress occurs via sticky Zimm and Rouse modes of the chains, hindered by the ionic bonds of a chain with oppositely charged neighboring chains. Because salt affects the bond energy of all ionic bonds to the same extent, all relaxation modes are shifted equally by adding salt. This gives rise to a generic relaxation spectrum for polyelectrolyte complex coacervates and other charge-driven soft materials.

■ ASSOCIATED CONTENT

● Supporting Information

Experimental details. This material is available free of charge via the Internet at <http://pubs.acs.org>.

■ AUTHOR INFORMATION

Corresponding Author

*E-mail jasper.vandergucht@wur.nl.

Notes

The authors declare no competing financial interest.

■ ACKNOWLEDGMENTS

E.S. and J.v.d.G. acknowledge financial support from The Netherlands Organisation for Scientific Research (NWO).

■ REFERENCES

- (1) Capito, R. M.; Azevedo, H. S.; Velichko, Y. S.; Mata, A.; Stupp, S. *I. Science* **2008**, *319*, 1812–1816.
- (2) Biesheuvel, P. M.; Mauser, T.; Sukhorukov, G. B.; Möhwald, H. *Macromolecules* **2006**, *39*, 8480–8486.
- (3) van der Kooij, H. M.; Spruijt, E.; Voets, I. K.; Fokkink, R.; Cohen Stuart, M. A.; van der Gucht, J. *Langmuir* **2012**, *28*, 14180–14191.
- (4) Martens, A. A.; van der Gucht, J.; Eggink, G.; de Wolf, F. A.; Cohen Stuart, M. A. *Soft Matter* **2009**, *5*, 4191–4197.
- (5) Lemmers, M.; Sprakel, J.; Voets, I. K.; van der Gucht, J.; Cohen Stuart, M. A. *Angew. Chem., Int. Ed.* **2010**, *49*, 708–711.
- (6) Stewart, R. J.; Wang, C. S.; Shao, H. *Adv. Colloid Interface Sci.* **2011**, *167*, 85–93.
- (7) Hwang, D. S.; Zeng, H.; Srivastava, A.; Krogstadt, D. V.; Tirrell, M.; Israelachvili, J. N.; Waite, J. H. *Soft Matter* **2010**, *6*, 3232–3236.
- (8) Clausell, J.; Happel, N.; Hale, T. K.; Doenecke, D.; Beato, M. *PLoS One* **2009**, *4*, e0007243.
- (9) Tavoosi, N.; Davis-Harrison, R. L.; Pogorelov, T. V.; Ohkubo, Y. Z.; Arcario, M. J.; Clay, M. C.; Rienstra, C. M.; Tajkhorshid, E.; Morrissey, J. H. *J. Biol. Chem.* **2011**, *286*, 23247–23253.
- (10) van der Gucht, J.; Spruijt, E.; Lemmers, M.; Cohen Stuart, M. A. *J. Colloid Interface Sci.* **2011**, *361*, 407–422.
- (11) Spruijt, E.; Westphal, A. H.; Borst, J. W.; Cohen Stuart, M. A.; van der Gucht, J. *Macromolecules* **2010**, *43*, 6476–6484.
- (12) Biesheuvel, P. M.; Cohen Stuart, M. A. *Langmuir* **2004**, *20*, 4764–4770.
- (13) Spruijt, E.; Sprakel, J.; Lemmers, M.; Cohen Stuart, M. A.; van der Gucht, J. *Phys. Rev. Lett.* **2010**, *105*, 208301.
- (14) Hone, J. H. E.; Howe, A. M.; Cosgrove, T. *Macromolecules* **2000**, *33*, 1199–1205.
- (15) Nikolaeva, O.; Budtova, T.; Brestkin, Y.; Zoolshoev, Z.; Frenkel, S. *J. Appl. Polym. Sci.* **1999**, *72*, 1523–1528.
- (16) Dreval, V. E.; Vasilév, G. B.; Litmanovich, E. A.; Kulichikhin, V. G. *Polym. Sci., Ser. A* **2008**, *50*, 751–756.
- (17) Bohidar, H. B.; Dubin, P. L.; Majhi, P. R.; Tribet, C.; Jaeger, W. *Biomacromolecules* **2005**, *6*, 1573–1585.
- (18) Weinbreck, F.; Wientjes, R. H. W.; Nieuwenhuijse, H.; Robijn, G. W.; De Kruif, C. G. *J. Rheol.* **2004**, *48*, 1215–1228.
- (19) Wang, X.; Lee, J.; Wang, Y.-W.; Huang, Q. *Biomacromolecules* **2007**, *8*, 992–997.
- (20) Baumgaertel, M.; Winter, H. H. *J. Non-Newtonian Fluid Mech.* **1992**, *44*, 15–36.
- (21) Baumgaertel, M.; Winter, H. H. *Rheol. Acta* **1989**, *28*, 511–519.
- (22) Mao, R.; Tang, J.; Swanson, B. G. *J. Food Sci.* **2000**, *65*, 374–381.
- (23) Hopkins, I. L.; Hamming, R. W. *J. Appl. Phys.* **1957**, *28*, 906–909.
- (24) Evans, R. M. L.; Tassieri, M.; Auhl, D.; Waigh, T. A. *Phys. Rev. E* **2009**, *80*, 012501.
- (25) Ferry, J. D. *Viscoelastic Properties of Polymers*; John Wiley & Sons: New York, 1980.
- (26) Rubinstein, M.; Colby, R. H. *Polymer Physics*; Oxford University Press: New York, 2003.
- (27) Archer, L. A. *J. Rheol.* **1999**, *43*, 1555–1571.
- (28) Rubinstein, M.; Semenov, A. N. *Macromolecules* **2001**, *34*, 1058–1068.
- (29) Spruijt, E.; van den Berg, S. A.; Cohen Stuart, M. A.; van der Gucht, J. *ACS Nano* **2012**, *6*, 5297–5303.
- (30) Loginova, D. V.; Lileev, A. S.; Lyashchenko, A. K. *Russ. J. Inorg. Chem.* **2002**, *47*, 1426–1433.
- (31) Milchev, A.; Binder, K. *Macromolecules* **1996**, *29*, 343–354.
- (32) Klein Wolterink, J.; Barkema, G. T.; Cohen Stuart, M. A. *Macromolecules* **2005**, *38*, 2009–2014.
- (33) Wong, J. S. S.; Hong, L.; Bae, S. C.; Granick, S. *Macromolecules* **2011**, *44*, 3073–3076.
- (34) Pawar, N.; Bohidar, H. B. *Phys. Rev. E* **2010**, *82*, 036107.
- (35) van den Burgh, S.; de Keizer, A.; Cohen Stuart, M. A. *Langmuir* **2004**, *20*, 1073–1084.
- (36) Lemmers, M.; Spruijt, E.; Beun, L.; Fokkink, R.; Leermakers, F. A. M.; Portale, G.; Cohen Stuart, M. A.; van der Gucht, J. *Soft Matter* **2012**, *8*, 104–117.
- (37) Chollakup, R.; Smitthipong, W.; Eisenbach, C. D.; Tirrell, M. *Macromolecules* **2010**, *43*, 2518–2528.